愛媛大学理学部紀要　第 22 巻　1–17 ページ，2019 年
Mem. Fac. Sci. Ehime Univ., vol. 22, p. 1–17, 2019

Intraspecific variations of the astragalar and calcaneal sizes in living Japanese monkey (*Macaca fuscata*)

現生ニホンザルにおける距骨および踵骨サイズの種内変異

Takehisa Tsubamoto
鍔本 武久

Earth's Evolution and Environment, Department of Mathematics, Physics, and Earth Sciences, Graduate School of Science and Engineering, Ehime University, 2-5 Bunkyo-cho, Matsuyama, Ehime Pref. 790-8577, Japan
愛媛大学 大学院理工学研究科 数理物質科学専攻 地球進化学講座

Abstract.

The intraspecific variations of the astragalar and calcaneal sizes of living Japanese monkey, *Macaca fuscata* (Mammalia, Primates, Cercopithecidae), were examined as an example to make basic data in considering the variations of fossil mammalian bones. The specimens examined consist of 478 individuals (233 adult specimens: 112 males and 121 females; 245 juvenile specimens: 142 males and 103 females). The data consist of 12 measurements for both the astragalus and calcaneum with body mass and molar sizes. Although there are sexual dimorphisms (male, larger; female, smaller) in all measurements of these two bones of the adult specimens, the distribution of each measurement is not clearly bimodal but generally unimodal. To see and compare the degree of variation, the coefficient of variation (CV) is calculated. CVs of the adult astragalar and calcaneal sizes range from 6.5 to 9.1 and from 6.9 to 10.8, respectively, implying that the variation of the calcaneal sizes appears to be slightly higher than that of the astragalar sizes as a whole. These CVs of the adult astragalar and calcaneal sizes are generally higher than those of the molars (4.9–6.6), implying that the intraspecific variations of these two bones are higher than those of the molars in *M. fuscata*. The principal component analyses indicated that the sexual dimorphisms of the adult astragalus and calcaneum were caused mostly by the overall size of the bones. The correlation coefficient between the body mass and each adult astragalar and calcaneal measurement ranges from 0.28 to 0.54, implying that the correlation between the body mass and the adult astragalar and calcaneal sizes in *M. fuscata* is not very high. The allometric correlation between the body mass and the astragalar and calcaneal sizes of the juvenile specimens are generally high.

Key words: Key words: astragalus, basic statistics, calcaneum, calcaneus, *Macaca fuscata*, Primates, talus

Introduction

Among mammalian bones, the astragalus (talus, ankle bone) and calcaneum (calcaneus, heel bone) are relatively well studied in terms of taxonomy, phylogeny, and functional morphology in primatology/physical anthropology (Gebo *et al*., 1991, 2000, 2001; Dagosto and Terranova, 1992; Rafferty *et al*., 1995; Nakatsukasa *et al*., 1997; Seiffert and Simons, 2001; Ciochon *et al*., 2001; Gunnell *et al*., 2002; Marivaux *et al*., 2003, 2010; Ciochon and Gunnell, 2004; Gebo and Dagosto, 2004; Gunnell and Ciochon, 2008; Dagosto *et al*., 2010; Parr *et al*., 2011; Hébert *et al*., 2012; Jogahara and Natori, 2013; Tsubamoto *et al*., 2016; Tsubamoto, 2019), paleontology (Szalay, 1977; Martinez and Sudre 1995; Penkrot *et al*., 2008; Bergqvist, 2008; Shockey and Anaya, 2008; Polly, 2008; Boyer and Bloch, 2008; Tsubamoto, 2014), and archaeozoology (DeGusta and Vrba, 2003; Plummer *et al*., 2008). Nevertheless, studies that precisely investigated the intraspecific variations of these two bones are few, so that the criteria or standards to discuss the intra- and inter-specific variations of these two bones in fossil mammals are still not very clear.

In this material report, as an example, I investigated intraspecific variations of the astragalar and calcaneal sizes in living Japanese monkey, *Macaca fuscata* (Gray, 1870) (Mammalia, Primates, Cercopithecidae), to provide basic data in considering the variations of fossil

2019 年 1 月 11 日 受付　　2019 年 4 月 24 日 受理
2019 年 5 月 1 日 発行
Received: 11 January, 2019; Accepted: 24 April, 2019
Published: 1 May, 2019

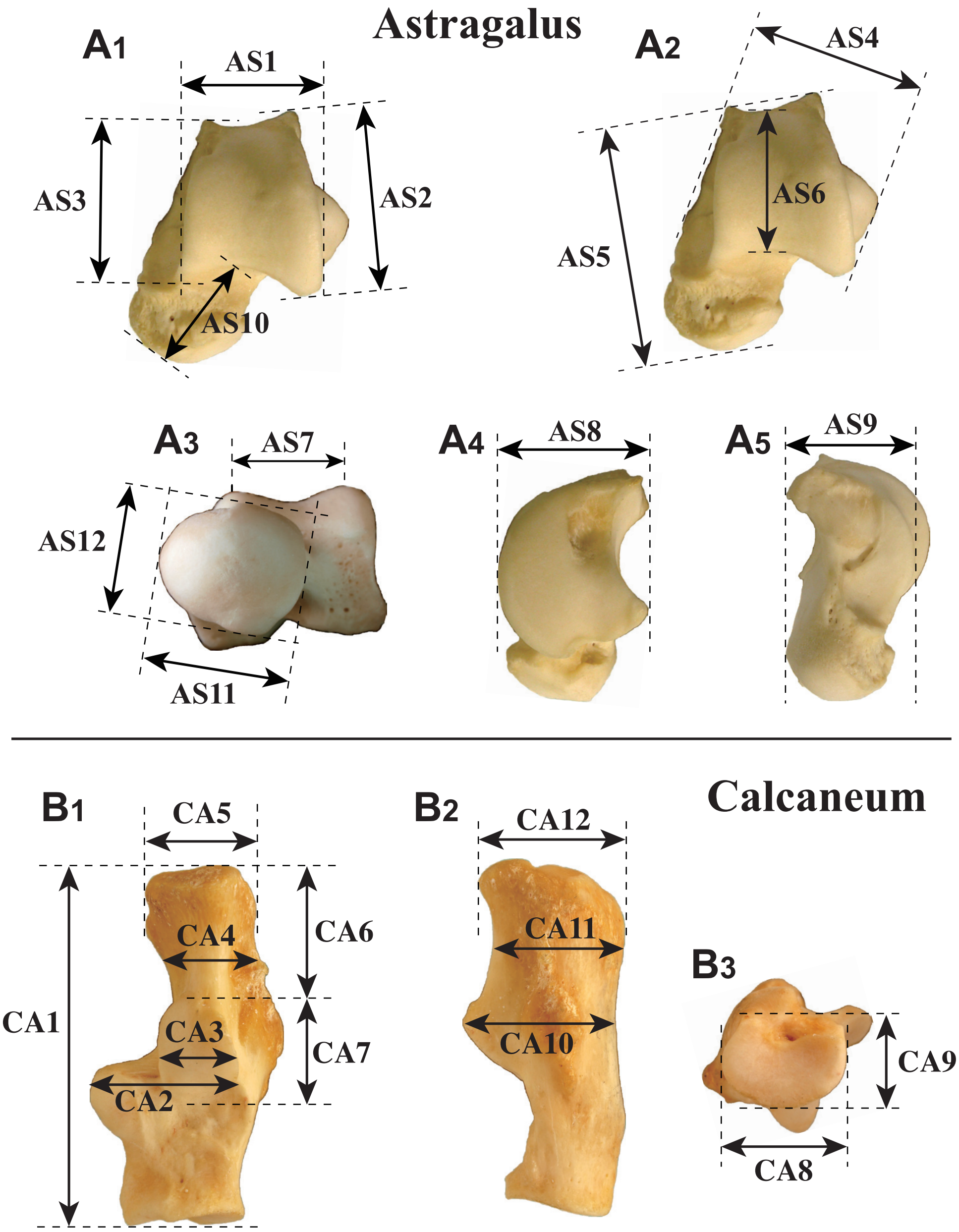

Figure 1. Measurement positions of the astragalus and calcaneum of *Macaca fuscata* (Primates, Catarrhini, Cercopithecidae) used in this study (after Tsubamoto, 2014, 2019; Tsubamoto *et al*., 2016). **A**, left astragalus: A_1–A_2, dorsal (anterior) view; A_3, distal view; A_4, lateral view; A_5, medial view. *Linear measurements*.—AS1, medio-lateral width of the tibial trochlea; AS2, proximo-distal length of the lateral trochlear ridge of the tibial trochlea; AS3, proximo-distal length of the medial trochlear ridge of the tibial trochlea; AS4, medio-lateral width of the astragalus; AS5, proximo-distal length of the astragalus; AS6, proximo-distal length of the central part of the tibial trochlea; AS7, medio-lateral width between the medial and lateral trochlear ridges of the tibial trochlea; AS8, dorso-ventral thickness of the lateral part of the astragalus; AS9, dorso-ventral thickness of the medial part of the astragalus; AS10, neck-head length; AS11, width of the head; AS12, thickness of the head. **B**, left calcaneum: B_1, dorsal (anterior) view; B_2, lateral view; B_3, distal view. *Linear measurements*.—CA1, calcaneal length; CA2, calcaneal width at the astragalar articular surfaces; CA3, width of the posterior astragalar articular surface; CA4, width of the posterior calcaneal body; CA5, width of the tuberosity; CA6, length of the posterior calcaneal body; CA7, length of the posterior astragalar articular surface; CA8, width of the articular surface for the cuboid; CA9, height of the articular surface for the cuboid; CA10, height at the posterior astragalar articular surface; CA11, height at the posterior calcaneal body; CA12, height at the tuberosity.

mammalian bones. *M. fuscata* was chosen as an example because it is well studied (*e.g.*, Fooden and Aimi, 2005) and because many of its skeletal specimens are stored in Japan.

Material and methods

The original data were taken from the skeletal specimens of the subspecies *Macaca fuscata fuscata* stored in Primate Research Institute, Kyoto University, Inuyama, Japan. The specimens used here consist of 478 individuals (233 adult specimens, 112 males and 121 females; 245 juvenile specimens, 142 males and 103 females) (Appendix Table A1). These specimens are chosen randomly as much as possible in the instutute. The specimens having erupted third molars and/or fused epiphyses of the long limb bones were identified as of adult individuals. The juvenile specimens here mean non-adult ones. For each astragalus and calcaneum, 12 measurements were taken (Figure 1). For comparison, the body mass and length and width of the molars of the individuals were also measured, and the body mass of each individual was taken from the data base of the institute. The units of the linear measurements and body mass are millimeter (mm) and gram (g), respectively. The linear measurements were taken to the nearest of 0.01 mm using digital calipers and were measured mostly on the left side when available. The analyses were carried out mostly using Excel (Microsoft) and JMP (SAS Institute Inc.), with VISUAL-SILVERMAN (Kusuhashi and Okamoto, 2015) for Silverman's test and R ver. 3.5.1 (Ihaka and Gentleman, 1996; R Core Team, 2018) for multivariate allometry.

Abbreviations.—AS1–AS12, measurement points of the astragalus (Figure 1A); CA1–CA12, measurement points of the calcaneum (Figure 1B); CV, coefficient of variation (unbiased); M1–M3/m1–m3, upper/lower molars; PC1, first principal component; PC2, second principal component; PCA, principal component analysis; adjusted R^2, coefficients of determination adjusted to the number of variables; RMA, reduced major axis.

Table 1. Basic statistics of the body mass (in gram) of the adult specimens. V, variance (unbiased); SD, standard deviation (unbiased); SE, standard error (unbiased); Max, maximal value; Min, minimal value; N, sample size.

	Adult all	Adult male	Adult female
V	6,262,269	5,216,556	2,704,276
SD	2,502	2,284	1,644
SE	164	216	149
Mean	8,587	10,183	7,110
Median	8,500	10,000	7,000
Max	16,500	16,500	11,400
Min	3,200	5,300	3,200
Skewness	0.50	0.28	0.11
Kurtosis	0.15	0.27	-0.31
N	233	112	121

Results and remarks

Adult specimens

The basic statistics and distributions of all the measurements of adult specimens are shown in Tables 1–4, Figures 2–5, and Appendix Figures A1–A2.

Size distribution and sexual dimorphism.—According to Welch's t test (5% significance level), there are significant differences between males and females (sexual dimorphisms: male, larger; female, smaller) in all adult measurements of the body mass, astragalus, calcaneum, and molars (Appendix Figures A1–A2). However, each size distribution of the adult measurements including the body mass and molars is superficially unimodal generally (Figures 2–4). The tests of the normality for the linear measurements and lognormality for the body mass (5% significance level) were applied to each measurement. Most of the measurements could

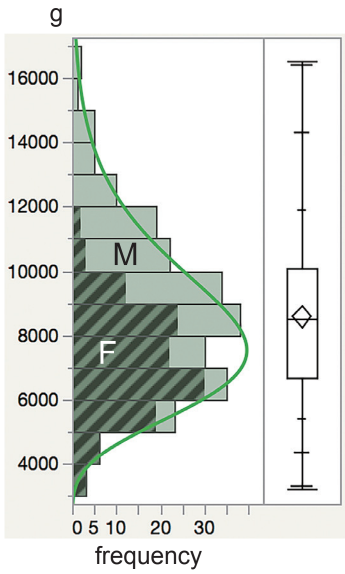

Figure 2. Histogram and box plot of the body mass of the adult specimens. The box plot shows quartiles with arithmetic mean (diamond) and whiskers from minimum to maximum with 0.5th, 2.5th, 10th, 90th, 97.5th, and 99.5th percentiles. Green line indicates the fitting for lognormal distribution. F, female; M, male.

Table 2. Basic statistics of the astragalar measurements (in mm) of the adult specimens. AS1–AS12, measurement points of the astragalus shown in Figure 1A; CV, coefficient of variation (unbiased). Other abbreviations are indicated in Table 1.

Adult all	AS1	AS2	AS3	AS4	AS5	AS6	AS7	AS8	AS9	AS10	AS11	AS12
CV	7.20	7.44	6.96	8.08	6.50	7.29	7.85	7.04	7.68	8.19	8.12	9.08
V	0.84	1.33	1.08	2.02	2.37	0.91	0.61	0.80	0.94	1.17	0.85	0.78
SD	0.91	1.15	1.04	1.42	1.54	0.96	0.78	0.89	0.97	1.08	0.92	0.89
SE	0.060	0.076	0.068	0.093	0.101	0.063	0.051	0.059	0.064	0.071	0.060	0.058
Mean	12.70	15.50	14.95	17.60	23.66	13.12	9.95	12.68	12.64	13.20	11.34	9.75
Median	12.72	15.48	14.92	17.53	23.65	13.07	9.98	12.65	12.54	13.22	11.32	9.70
Max	15.17	18.40	17.56	23.72	27.38	16.15	12.24	15.04	15.11	15.79	14.18	14.14
Min	10.61	11.56	12.58	13.98	19.32	9.72	8.15	10.03	10.26	10.04	8.99	7.93
Skewness	-0.07	-0.03	0.16	0.48	0.09	-0.06	-0.11	0.08	0.26	-0.04	0.13	0.80
Kurtosis	-0.67	0.17	-0.41	1.16	-0.48	0.25	-0.26	-0.32	-0.56	-0.31	0.01	2.47
N	233	233	233	233	233	233	233	233	233	233	233	233

Adult male	AS1	AS2	AS3	AS4	AS5	AS6	AS7	AS8	AS9	AS10	AS11	AS12
CV	4.55	5.51	5.48	6.50	4.37	5.70	5.34	5.23	5.60	6.00	5.47	7.79
V	0.37	0.80	0.73	1.44	1.17	0.61	0.31	0.48	0.56	0.70	0.43	0.64
SD	0.61	0.90	0.86	1.20	1.08	0.78	0.56	0.69	0.75	0.83	0.65	0.80
SE	0.057	0.085	0.081	0.113	0.102	0.074	0.053	0.066	0.071	0.079	0.062	0.076
Mean	13.38	16.27	15.62	18.48	24.82	13.73	10.45	13.28	13.36	13.91	11.97	10.27
Median	13.43	16.21	15.70	18.37	24.88	13.79	10.44	13.26	13.43	13.90	11.93	10.13
Max	15.17	18.40	17.56	23.72	27.38	16.15	12.24	15.04	15.11	15.79	14.18	14.14
Min	11.65	13.89	13.24	16.42	22.30	11.63	9.06	11.47	11.58	12.07	10.71	8.90
Skewness	-0.13	0.03	0.00	1.06	0.11	-0.11	0.32	0.02	-0.07	-0.03	0.55	1.40
Kurtosis	0.27	0.08	-0.19	3.13	0.06	0.45	0.74	-0.05	0.02	-0.26	0.39	4.59
N	112	112	112	112	112	112	112	112	112	112	112	112

Adult female	AS1	AS2	AS3	AS4	AS5	AS6	AS7	AS8	AS9	AS10	AS11	AS12
CV	5.59	5.82	5.48	6.55	4.64	5.78	6.92	5.50	5.12	6.73	6.81	7.16
V	0.46	0.74	0.62	1.21	1.10	0.53	0.43	0.44	0.38	0.71	0.54	0.44
SD	0.68	0.86	0.78	1.10	1.05	0.73	0.66	0.67	0.61	0.84	0.73	0.66
SE	0.061	0.078	0.071	0.100	0.095	0.066	0.060	0.061	0.056	0.077	0.067	0.060
Mean	12.08	14.78	14.33	16.80	22.60	12.55	9.48	12.12	11.97	12.54	10.76	9.27
Median	12.08	14.85	14.27	16.81	22.55	12.63	9.53	12.14	11.91	12.58	10.73	9.33
Max	13.71	17.38	16.59	20.51	25.09	14.31	10.76	14.18	14.07	14.77	13.78	11.73
Min	10.61	11.56	12.58	13.98	19.32	9.72	8.15	10.03	10.26	10.04	8.99	7.93
Skewness	0.17	-0.47	0.18	0.26	0.06	-0.62	0.00	0.06	0.33	-0.17	0.53	0.36
Kurtosis	-0.23	1.48	-0.04	0.22	0.18	0.98	-0.78	0.36	0.88	-0.15	2.07	1.23
N	121	121	121	121	121	121	121	121	121	121	121	121

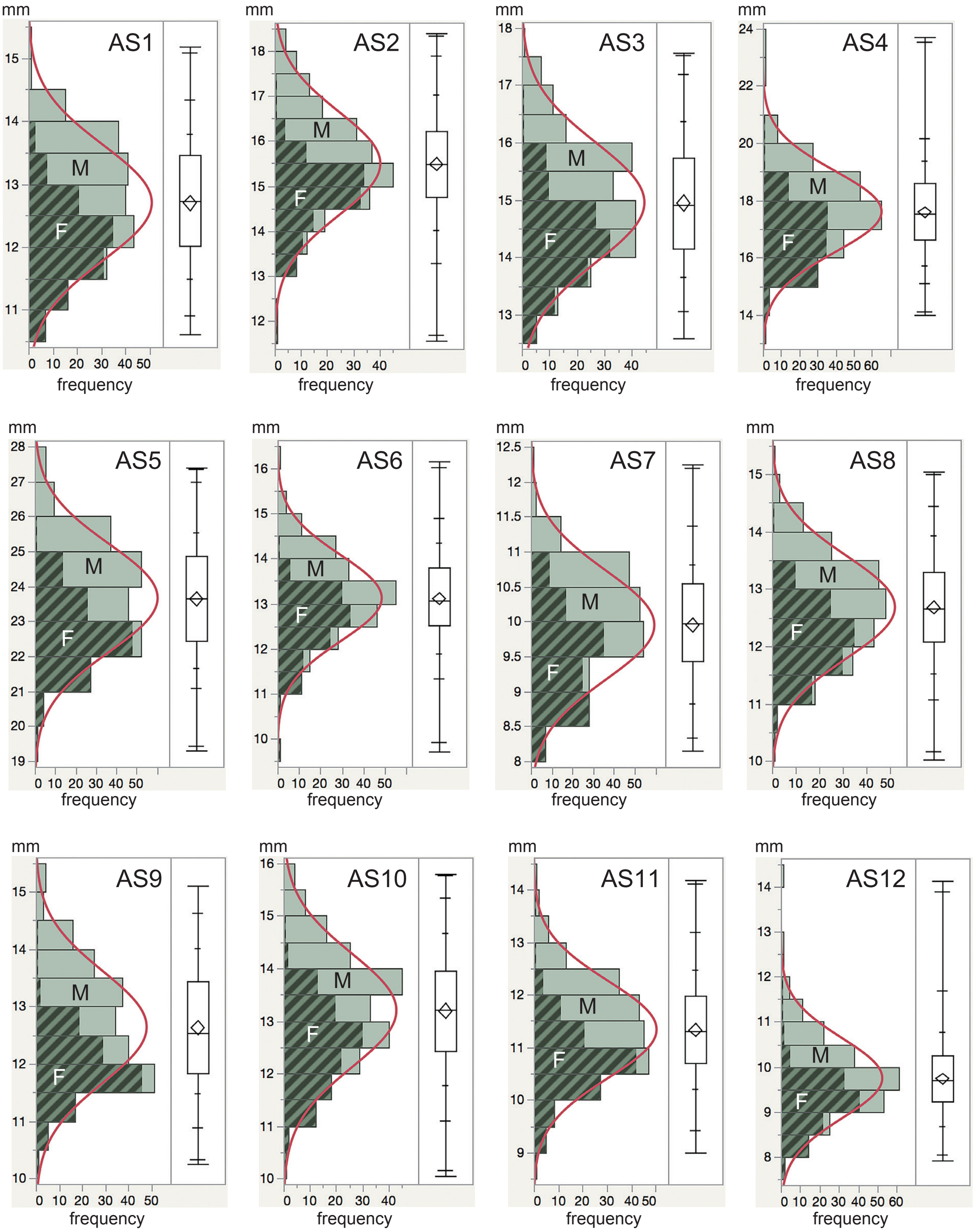

Figure 3. Histograms and box plots of the astragalar measurements of the adult specimens. Red line indicates the fitting for the normal distribution. Other abbreviations are shown in Figures 1–2.

Table 3. Basic statistics of the calcaneal measurements (in mm) of the adult specimens. CA1–CA12, measurement points of the calcaneum shown in Figure 1B. Other abbreviations are indicated in Tables 1–2.

Adult all	CA1	CA2	CA3	CA4	CA5	CA6	CA7	CA8	CA9	CA10	CA11	CA12
CV	6.97	7.20	9.13	10.81	8.65	10.20	9.00	6.89	8.71	7.66	7.76	8.68
V	6.36	1.43	0.65	0.79	0.91	1.70	1.03	0.68	0.55	1.40	1.09	1.95
SD	2.52	1.20	0.81	0.89	0.96	1.30	1.02	0.82	0.74	1.18	1.04	1.40
SE	0.167	0.079	0.053	0.059	0.063	0.086	0.067	0.054	0.049	0.078	0.069	0.092
Mean	36.19	16.63	8.85	8.20	11.04	12.80	11.29	11.93	8.50	15.46	13.44	16.10
Median	36.01	16.61	8.81	8.16	10.90	12.82	11.24	11.89	8.47	15.33	13.39	16.03
Max	43.09	20.46	11.23	11.08	13.69	16.84	14.18	14.42	10.72	18.71	16.07	19.84
Min	30.46	13.80	6.97	6.07	9.07	9.36	9.08	10.02	6.38	12.54	10.60	13.14
Skewness	0.15	0.15	0.26	0.30	0.40	-0.12	0.34	0.29	0.29	0.23	0.25	0.31
Kurtosis	-0.41	-0.26	-0.08	-0.26	-0.32	-0.03	-0.03	-0.24	0.23	-0.15	-0.11	-0.12
N	229	229	229	229	229	229	229	229	229	229	229	229

Adult male	CA1	CA2	CA3	CA4	CA5	CA6	CA7	CA8	CA9	CA10	CA11	CA12
CV	4.76	5.64	7.41	8.81	7.09	7.07	8.42	4.91	7.56	6.09	6.61	7.48
V	3.28	0.96	0.47	0.60	0.68	0.93	0.98	0.38	0.45	0.98	0.86	1.60
SD	1.81	0.98	0.69	0.77	0.83	0.96	0.99	0.61	0.67	0.99	0.93	1.26
SE	0.173	0.093	0.066	0.074	0.079	0.092	0.094	0.059	0.064	0.094	0.089	0.120
Mean	38.05	17.35	9.28	8.78	11.66	13.63	11.75	12.52	8.87	16.25	14.05	16.89
Median	37.82	17.32	9.19	8.78	11.70	13.61	11.60	12.49	8.82	16.25	14.01	16.90
Max	43.09	20.46	11.04	11.08	13.69	16.84	14.18	14.42	10.72	18.71	16.04	19.84
Min	34.20	15.10	7.61	6.86	9.80	11.19	9.54	11.29	7.04	13.61	11.68	13.61
Skewness	0.33	0.12	0.21	-0.19	0.15	0.18	0.31	0.41	0.35	0.12	0.04	0.15
Kurtosis	-0.17	0.12	-0.28	0.72	-0.19	0.63	-0.41	0.09	0.36	-0.17	-0.48	-0.08
N	110	110	110	110	110	110	110	110	110	110	110	110

Adult female	CA1	CA2	CA3	CA4	CA5	CA6	CA7	CA8	CA9	CA10	CA11	CA12
CV	5.02	6.09	8.33	7.83	6.38	9.07	7.73	5.13	7.66	5.59	6.22	7.04
V	3.00	0.95	0.50	0.36	0.45	1.19	0.70	0.34	0.39	0.68	0.64	1.17
SD	1.73	0.97	0.70	0.60	0.67	1.09	0.84	0.58	0.62	0.82	0.80	1.08
SE	0.159	0.089	0.065	0.055	0.061	0.100	0.077	0.054	0.057	0.075	0.073	0.099
Mean	34.46	15.96	8.45	7.66	10.47	12.03	10.86	11.39	8.15	14.73	12.88	15.36
Median	34.50	15.81	8.41	7.67	10.43	12.13	10.93	11.34	8.18	14.75	12.89	15.35
Max	39.23	19.32	11.23	9.46	12.43	15.24	12.96	13.85	9.95	17.03	16.07	18.97
Min	30.46	13.80	6.97	6.07	9.07	9.36	9.08	10.02	6.38	12.54	10.60	13.14
Skewness	0.07	0.34	0.63	0.36	0.50	-0.11	0.07	0.66	0.26	-0.16	0.23	0.28
Kurtosis	-0.21	0.36	1.45	0.62	0.41	-0.02	-0.20	2.11	0.49	0.15	1.57	0.30
N	119	119	119	119	119	119	119	119	119	119	119	119

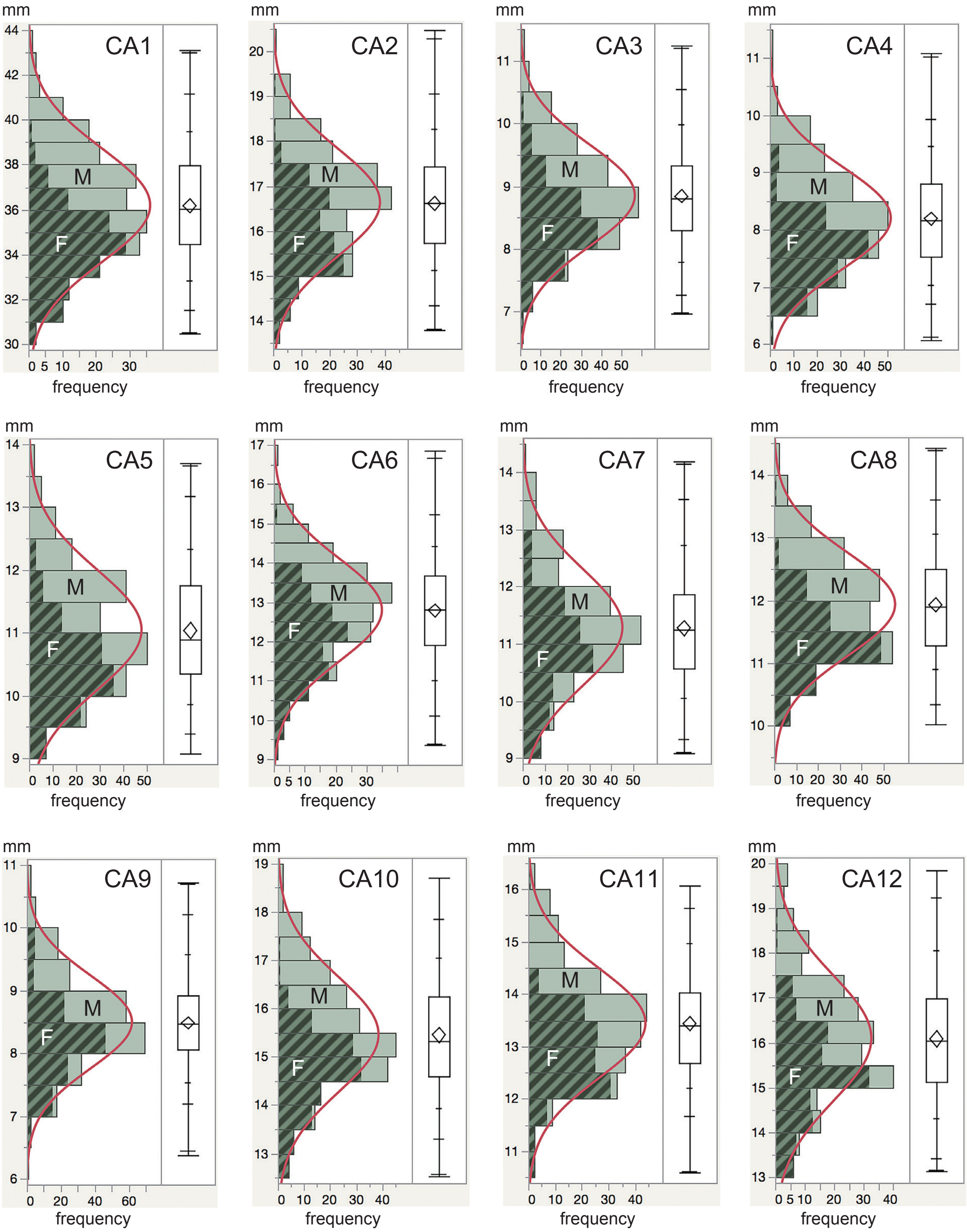

Figure 4. Histograms and box plots of the calcaneal measurements of the adult specimens. Abbreviations are shown in Figures 1–3.

Table 4. Basic statistics of the molar measurements (in mm) of the adult specimens. M1–M3/m1–m3, upper/lower molars; L, maximal length; W, maximal width. Other abbreviations are indicated in Table 1–2.

Adult all	M1 L	M1 W	M2 L	M2 W	M3 L	M3 W	m1 L	m1 W	m2 L	m2 W	m3 L	m3 W
CV	4.92	5.16	5.78	5.49	6.37	5.57	6.03	5.47	5.83	6.07	6.61	6.07
V	0.15	0.16	0.28	0.25	0.35	0.25	0.21	0.11	0.27	0.21	0.58	0.22
SD	0.39	0.40	0.53	0.50	0.59	0.50	0.46	0.34	0.52	0.45	0.76	0.47
SE	0.027	0.027	0.036	0.033	0.040	0.034	0.031	0.023	0.035	0.031	0.051	0.032
Mean	7.99	7.78	9.17	9.05	9.33	9.00	7.69	6.19	8.93	7.48	11.55	7.73
Median	7.98	7.76	9.17	9.05	9.35	8.96	7.67	6.21	8.95	7.48	11.51	7.73
Max	9.12	9.65	10.39	10.35	11.30	10.45	8.74	7.13	10.20	8.98	13.74	9.63
Min	7.02	6.68	7.93	7.77	7.61	7.68	6.54	5.29	7.86	6.26	9.16	6.27
Skewness	0.04	0.48	-0.08	-0.02	0.12	0.15	-0.07	0.03	0.12	0.40	0.04	0.31
Kurtosis	-0.26	1.65	-0.38	-0.18	0.68	0.06	-0.26	-0.10	-0.28	0.40	0.29	1.14
N	219	219	222	221	221	220	219	219	221	221	220	221

Adult male	M1 L	M1 W	M2 L	M2 W	M3 L	M3 W	m1 L	m1 W	m2 L	m2 W	m3 L	m3 W
CV	4.29	4.46	5.25	4.14	5.47	4.58	5.25	4.97	4.87	5.76	5.48	5.27
V	0.12	0.13	0.24	0.15	0.27	0.18	0.42	0.32	0.45	0.44	0.65	0.42
SD	0.35	0.36	0.49	0.39	0.52	0.42	0.17	0.10	0.20	0.20	0.43	0.18
SE	0.034	0.034	0.047	0.037	0.050	0.041	0.040	0.031	0.043	0.043	0.063	0.041
Mean	8.18	8.00	9.37	9.33	9.56	9.27	7.93	6.34	9.17	7.69	11.90	7.97
Median	8.24	7.97	9.31	9.29	9.51	9.23	7.99	6.35	9.13	7.65	11.84	7.95
Max	9.12	9.65	10.39	10.35	11.30	10.45	8.74	7.13	10.20	8.98	13.74	9.63
Min	7.27	7.33	7.96	8.46	8.09	8.22	6.76	5.43	8.22	6.69	10.46	6.96
Skewness	-0.04	1.14	-0.27	0.31	0.43	0.37	-0.28	-0.17	0.33	0.34	0.26	0.72
Kurtosis	-0.30	3.20	0.20	-0.21	1.76	0.23	-0.18	0.47	-0.20	0.47	-0.25	1.89
N	108	108	108	108	107	107	106	106	107	107	107	107

Adult female	M1 L	M1 W	M2 L	M2 W	M3 L	M3 W	m1 L	m1 W	m2 L	m2 W	m3 L	m3 W
CV	4.43	4.31	5.50	5.00	6.36	4.90	5.13	4.82	5.54	4.98	6.34	5.35
V	0.12	0.11	0.24	0.19	0.34	0.18	0.15	0.08	0.23	0.13	0.50	0.16
SD	0.35	0.33	0.49	0.44	0.58	0.43	0.38	0.29	0.48	0.36	0.71	0.40
SE	0.033	0.031	0.046	0.041	0.054	0.040	0.036	0.027	0.045	0.034	0.067	0.038
Mean	7.81	7.57	8.98	8.78	9.11	8.74	7.46	6.04	8.70	7.27	11.21	7.51
Median	7.84	7.56	8.99	8.73	9.08	8.68	7.51	6.04	8.69	7.27	11.25	7.54
Max	8.83	8.38	10.24	9.96	10.95	9.85	8.41	6.81	9.99	8.14	13.52	8.77
Min	7.02	6.68	7.93	7.77	7.61	7.68	6.54	5.29	7.86	6.26	9.16	6.27
Skewness	0.10	-0.04	0.06	0.14	0.17	0.16	-0.26	-0.00	0.25	0.08	0.13	0.02
Kurtosis	0.08	-0.10	-0.54	-0.05	0.25	0.10	-0.09	-0.27	-0.41	-0.22	1.03	0.73
N	111	111	114	113	114	113	113	113	114	114	113	114

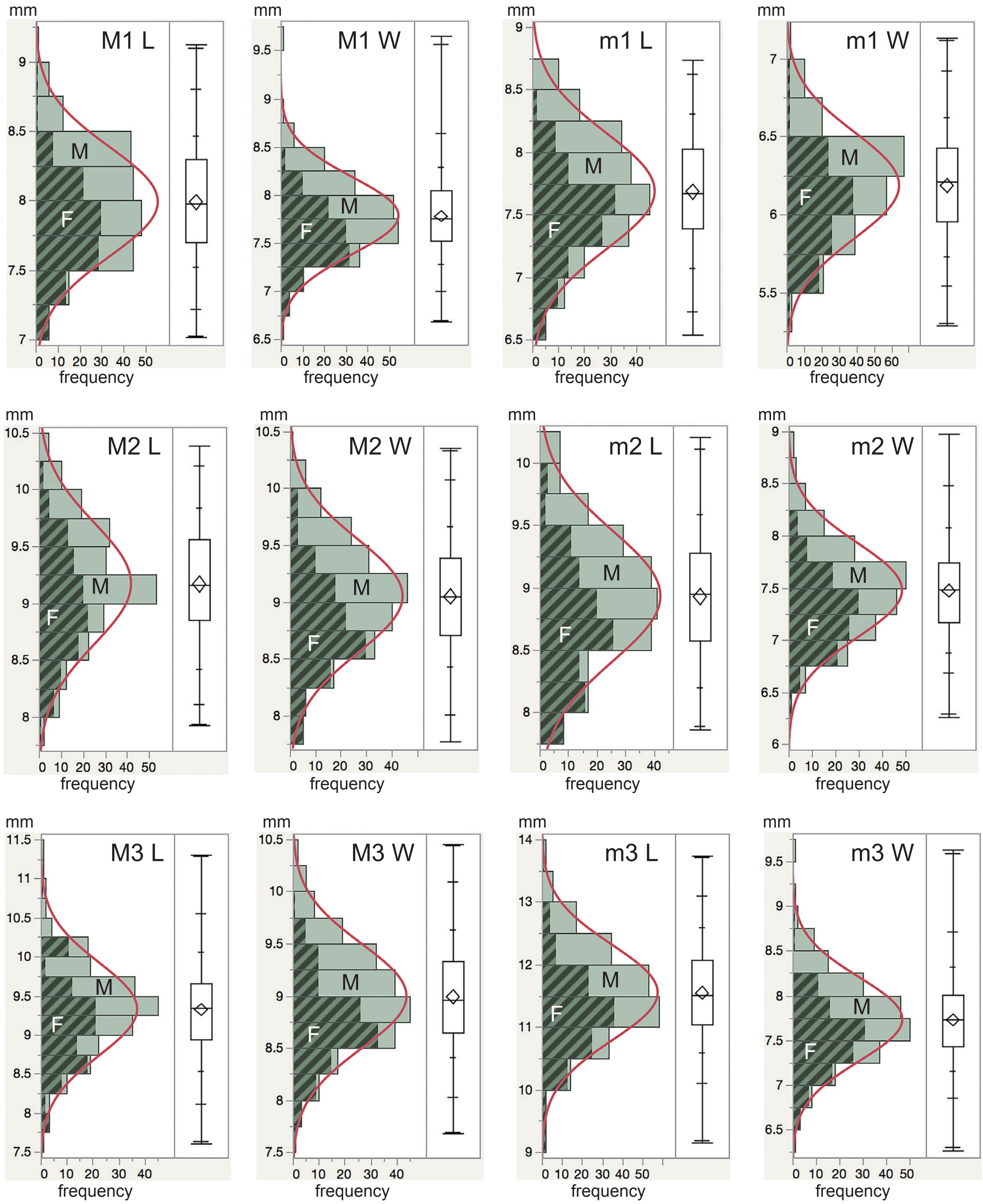

Figure 5. Histograms and box plots of the molar measurements of the adult specimens. M1–M3/m1–m3, upper/lower molars; L, maximal length; W, maximal width. Other abbreviations are shown in Figures 2–3.

not reject the null hypothesis, but some measurements rejected it (Table 5). To test the multimodality of each adult measurement, Silverman's test (5% significance level) (Silverman, 1981, 1983) was applied. Most of the adult measurements could not reject the unimodal hypothesis, but two measurements (AS5 and width of M1) rejected the unimodal hypothesis and could not reject the bimodal hypothesis. The possible bimodality of the width of M1 is caused by the upper outlier (Figure 5; Appendix Figure A2). Although the possible bimodality of AS5 was implied by Silverman's test, the normality of the distribution of AS5 was not rejected (Table 5). In any case, we can see no clear bimodality in each size distribution of the adult specimens (Figures 2–5). This result may suggest that if the size distributions of any astragalus, calcaneum, or molars of fossil adult primates show clear multimodalities, the differences appear to be caused not by a sexual dimorphism but by an interspecific variation. This hypothesis must be tested in examining specimens on more diverse species.

Coefficient of variation.—To see and compare the degree of variation, CV is calculated. CV of the adult astragalar and calcaneal sizes ranges from 6.5 to 9.1 and from 6.9 to 10.8, respectively (Tables 2–4). If we calculate CV separating the adult specimens into males and females, CV of the adult astragalar and calcaneal sizes ranges from 4.4 to 7.8 and from 4.8 to 9.1, respectively. CVs of the adult astragalar and calcaneal sizes are generally higher than those of the molars (all adult, 4.9–6.6; separating males and females, 4.1–6.3; Tables 2–4). This implies that the variations of the calcaneal sizes in *M. fuscata* are roughly as high as those of the astragalar sizes and that the variations of these two bones are higher than those of the molars in *M. fuscata*.

PCA and sexual dimorphism.—PCA using covariance matrices indicated that sexual dimorphisms of the adult astragalus and calcaneum are mostly caused by the overall size of each bone and had almost no other morphological differences (Figure 6). In the astragalus, the contribution rates of the PC1 and PC2 are *ca*. 80% and *ca*. 5%, respectively; in the calcaneum, they are *ca.* 74% and *ca*. 8%, respectively. In each case, the sexual dimorphism is explained mostly by the PC1, that is, their overall sizes.

Correlation with body mass.—The correlation coefficients between the body mass and the adult astragalar and calcaneal measurements are generally higher than those between the body mass and the molar measurements (Table 6; Appendix Figure A3). The correlation coefficient between the body mass and each adult astragalar measurement ranges from 0.38 to 0.54; that between the body mass and each adult calcaneal measurement ranges from 0.28 to 0.54 (Table 6). Therefore, the linear measurements of these two bones

Table 5. Goodness-of-fit tests of the fittings for the normal and lognormal distributions of the adult specimens. The normal test is for the linear measurements and the lognormal test is for the body mass (BM). The Shapiro-Wilk and the Kolmogorov-Smirnov tests were used for the tests of normality and lognormality, respectively. *, p-value < 0.05; **, p-value < 0.01. Other abbreviations are shown in Figure 1 and Tables 1–4.

	Normality (p-value)	Lognormality (p-value)
BM	—	0.0313*
AS1	0.0413*	—
AS2	0.6877	—
AS3	0.2607	—
AS4	0.0038**	—
AS5	0.0682	—
AS6	0.7305	—
AS7	0.0439	—
AS8	0.6740	—
AS9	0.0045**	—
AS10	0.7618	—
AS11	0.8958	—
AS12	<0.0001**	—
CA1	0.4655	—
CA2	0.5025	—
CA3	0.2990	—
CA4	0.0442*	—
CA5	0.0053**	—
CA6	0.7768	—
CA7	0.0309*	—
CA8	0.1298	—
CA9	0.1872	—
CA10	0.3209	—
CA11	0.0581	—
CA12	0.0587	—
M1 L	0.7499	—
M1 W	0.0071**	—
M2 L	0.2292	—
M2 W	0.9386	—
M3 L	0.1201	—
M3 W	0.8213	—
m1 L	0.4790	—
m1 W	0.5945	—
m2 L	0.1455	—
m2 W	0.0689	—
m3 L	0.7681	—
m3 W	0.1074	—

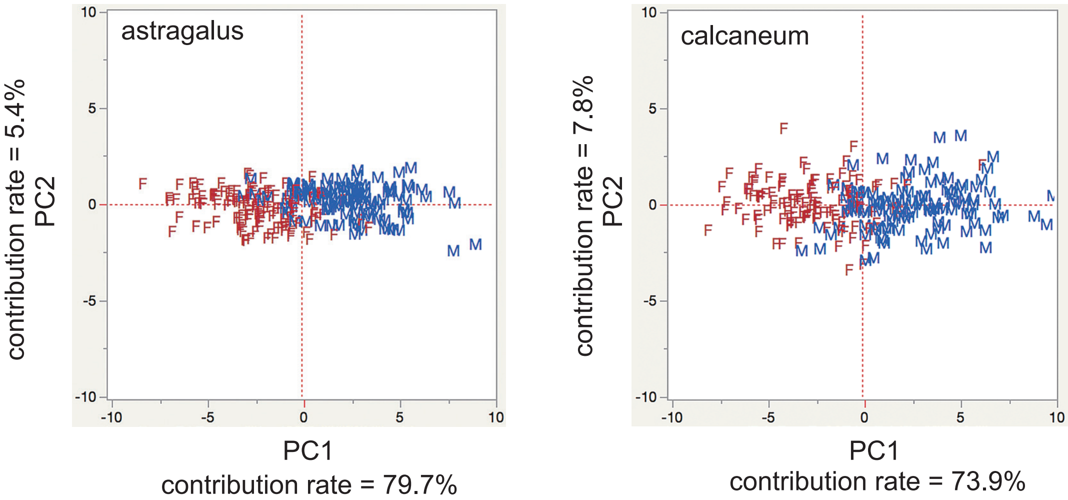

No.	eigen-value	contri-bution rate (%)
1	10.9	79.7
2	0.7	5.4

Eigenvector

	PC1	PC2
AS1	0.256	-0.034
AS2	0.324	-0.191
AS3	0.281	-0.005
AS4	0.395	-0.340
AS5	0.435	0.179
AS6	0.270	-0.125
AS7	0.199	-0.041
AS8	0.248	0.043
AS9	0.277	-0.023
AS10	0.222	0.885
AS11	0.248	-0.040
AS12	0.209	-0.098

No.	eigen-value	contri-bution rate (%)
1	13.7	73.9
2	1.4	7.8

Eigenvector

	PC1	PC2
CA1	0.653	-0.502
CA2	0.265	0.074
CA3	0.161	0.159
CA4	0.180	0.250
CA5	0.213	0.211
CA6	0.275	-0.501
CA7	0.194	0.262
CA8	0.188	0.101
CA9	0.135	0.118
CA10	0.290	0.228
CA11	0.237	0.301
CA12	0.304	0.352

Figure 6. Results of the principal component analysis using covariance matrices for all adult specimens of the astragalus (AS1–AS12) and calcaneum (CA1–CA12) (Figure 1). PC1, the first principal component; PC2, the second principal component; red F, female; blue M, male.

are positively correlate with the body mass, although the correlation is not very high. Also, the correlation between the body mass and the adult astragalar and calcaneal sizes are slightly higher generally than that between the body mass and the molars (0.27–0.41). Therefore, in *M. fuscata* the differences of the body mass of the individuals can be roughly estimated from the differences of the astragalar and calcaneal sizes, although it is difficult to estimate precisely the differences of the body mass based on the differences of the sizes of these two bones.

Juvenile (non-adult) specimens

CA1 and CA6 can be measured for the specimens of which epiphysis is at least partly fused (Figure 1B). Therefore, the data of CA1 and CA6 of the juvenile specimens are biased toward the elder (larger) specimens, and many of the data of CA1 and CA6 in the juvenile specimens are lacking (Appendix Table A1). Hence, CA1 and CA6 are excluded from the analyses below because those data are not enough for the analyses.

Correlation with body mass.—The bivariate plots between the juvenile astragalar or calcaneal sizes and the body mass in natural log scale show that there are good positive allometric correlations between them (Figures 7–8; Table 7). Adjusted R^2 values of the least square axes between them are larger than 0.78; (Figures 7–8; Table 7). On the RMA slopes, no significant sexual dimorphism was observed. The RMA slopes (isometry = 3) except varies from 1.8 to 3.2 (Figures 7–8; Table 7), implying the differences of growth rate among the measurements.

Multivariate allometry.—The analysis of multivariate allometry (Jolicoeur, 1963; Corruccini, 1983) was applied for the juvenile astragalus and calcaneum, respectively. This analysis is sometimes used in primatology (Mouri and Nishimura, 2002; Natori, 2002a, 2002b). To the growth of the overall size of the astragalus, AS1, AS5, AS7, AS10–AS12 are undergrowth

Table 6. Pearson's correlation coefficient between the body mass and each measurements of the adult specimens. Abbreviations are shown in Figure 1 and Tables 1–4.

AS1	0.519
AS2	0.476
AS3	0.517
AS4	0.382
AS5	0.485
AS6	0.433
AS7	0.420
AS8	0.473
AS9	0.536
AS10	0.481
AS11	0.442
AS12	0.440
CA1	0.470
CA2	0.369
CA3	0.383
CA4	0.497
CA5	0.448
CA6	0.438
CA7	0.281
CA8	0.536
CA9	0.351
CA10	0.477
CA11	0.445
CA12	0.452

M1 L	0.290
M1 W	0.353
M2 L	0.245
M2 W	0.410
M3 L	0.240
M3 W	0.374
m1 L	0.363
m1 W	0.291
m2 L	0.269
m2 W	0.292
m3 L	0.311
m3 W	0.304

Table 7. Several values of the relationship between the body mass and each measurement of the all juvenile specimens. All measurement values are natural log-transformed. LSA, least square axis; adjusted R^2, coefficients of determination adjusted to the number of variables; RMA, reduced major axis, CL, confidence limit with significance level of 0.05.

	LSA adjusted R^2	RMA intercept	RMA slope	RMA slope lower CL	RMA slope upper CL
AS1	0.860	1.21	2.89	2.75	3.05
AS2	0.885	3.26	1.95	1.87	2.04
AS3	0.868	3.44	1.89	1.80	1.99
AS4	0.886	2.08	2.29	2.19	2.40
AS5	0.879	0.26	2.63	2.51	2.76
AS6	0.866	3.82	1.84	1.75	1.93
AS7	0.850	2.92	2.42	2.30	2.56
AS8	0.888	3.48	2.03	1.94	2.13
AS9	0.899	3.01	2.24	2.14	2.33
AS10	0.806	0.36	3.21	3.02	3.41
AS11	0.869	2.13	2.68	2.55	2.81
AS12	0.875	3.02	2.47	2.35	2.59
CA2	0.880	2.73	2.09	2.00	2.19
CA3	0.863	3.32	2.46	2.34	2.59
CA4	0.838	2.72	2.95	2.79	3.12
CA5	0.856	3.29	2.29	2.16	2.42
CA7	0.841	2.20	2.64	2.50	2.79
CA8	0.859	2.71	2.42	2.29	2.56
CA9	0.784	2.82	2.70	2.51	2.90
CA10	0.881	1.31	2.75	2.63	2.88
CA11	0.871	1.40	2.85	2.72	3.00
CA12	0.849	2.30	2.32	2.19	2.46

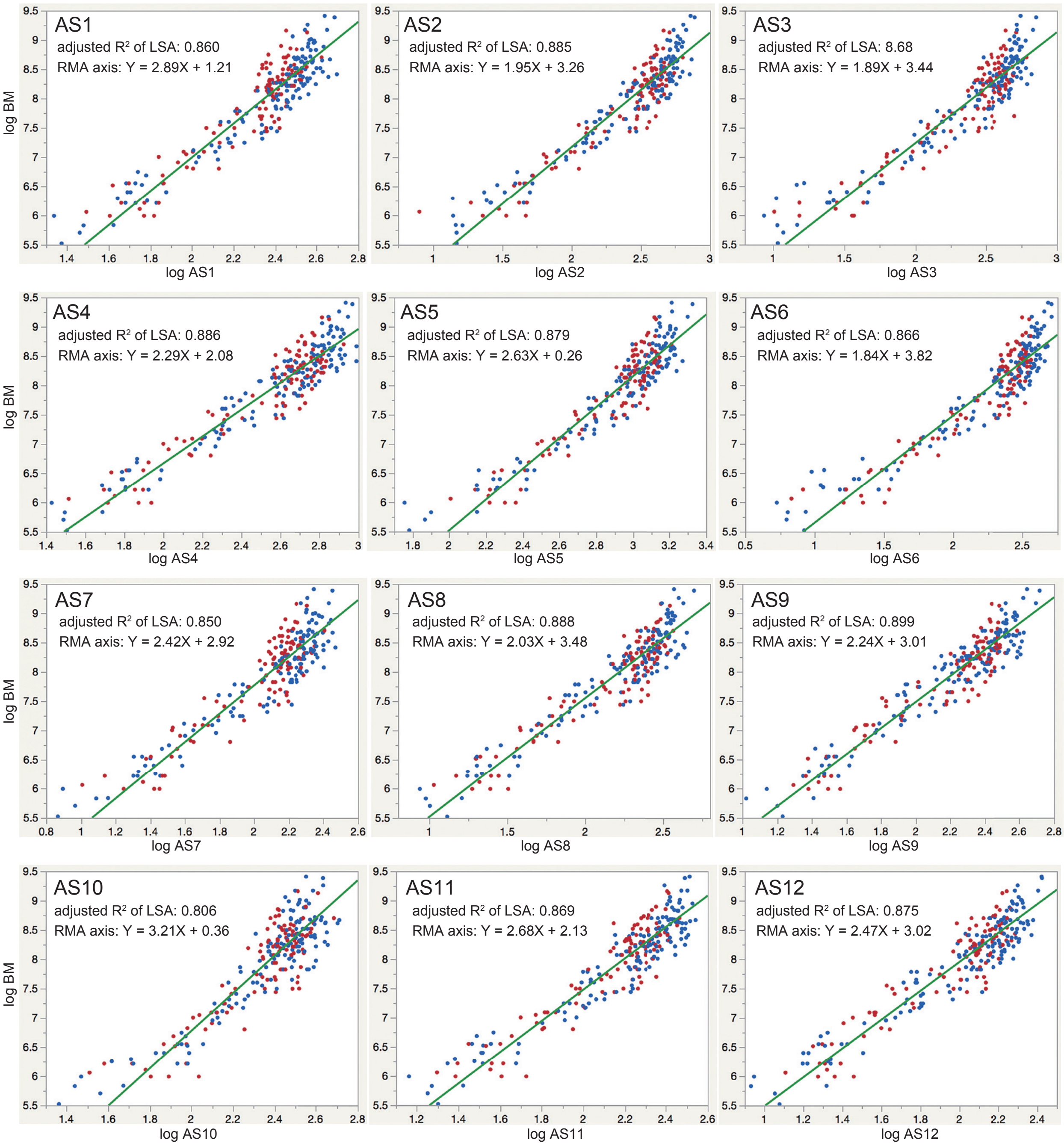

Figure 7. Scatter plots of body mass versus AS1–AS12 (Figure 1A) of the all juvenile specimens. All values are natural log-transformed. Red plots, female; blue plots, male; green line, reduced major axis (RMA); LSA, least square axis.

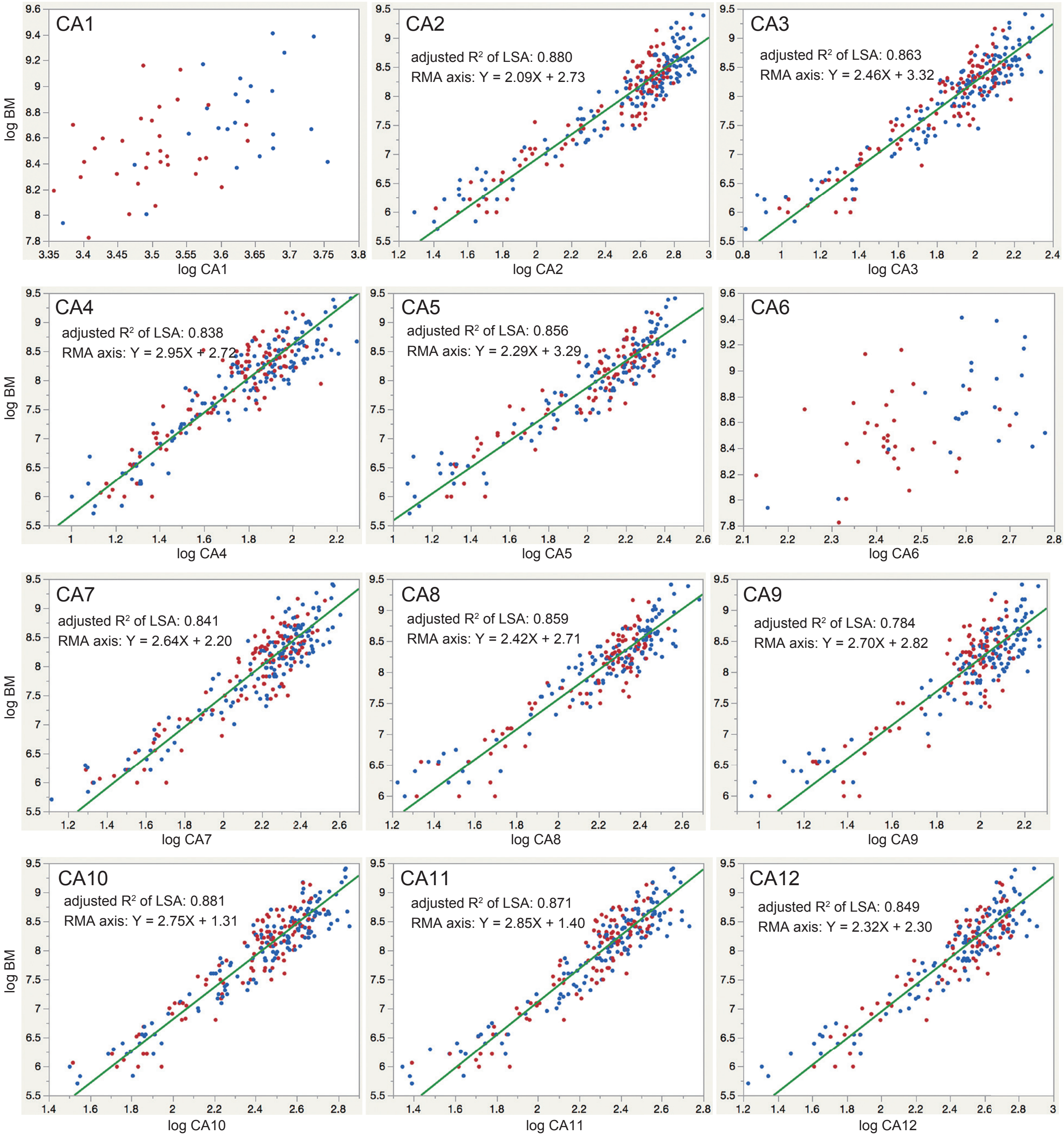

Figure 8. Scatter plots of body mass versus CA1–CA12 (Figure 1B) of the all juvenile specimens. All values are natural log-transformed. Other abbreviations are indicated in Figure 7.

Table 8. Allometry coefficients and their 95% upper and lower confidence limits divided by isometric value for the 12 measurements (AS1–AS12) of the astragalus and the 10 measurements (CA2–CA5 and CA7–CA12) of the calcaneum of the juvenile specimens. The isometric value for the astragalus is 1/√12; that for the calcaneum is 1/√10. In the table, isometry = 1.

	AS1	AS2	AS3	AS4	AS5	AS6	AS7	AS8	AS9	AS10	AS11	AS12
upper confidence limit	0.77	1.15	1.18	0.99	0.85	1.22	0.92	1.11	0.99	0.66	0.84	0.90
allometry coefficient divided by isometric value	0.79	1.17	1.21	1.00	0.87	1.25	0.94	1.13	1.02	0.69	0.85	0.92
lower confidence limit	0.80	1.20	1.23	1.01	0.89	1.28	0.96	1.15	1.05	0.72	0.87	0.95

	CA2	CA3	CA4	CA5	CA7	CA8	CA9	CA10	CA11	CA12
upper confidence limit	1.20	0.99	0.84	1.08	0.85	1.02	0.89	0.90	0.84	1.04
allometry coefficient divided by isometric value	1.22	1.01	0.87	1.11	0.89	1.05	0.93	0.92	0.86	1.07
lower confidence limit	1.24	1.03	0.91	1.15	0.92	1.08	0.96	0.95	0.89	1.09

(allometry coefficient < 1); AS4 and AS9 are isometric (~ 1); and AS2–AS3, AS6, and AS8 are overgrowth (> 1) (Table 8). As growing up, the proportion of the astragalus changes as follows: the length and neck shortens, the head becomes smaller, the trochlea becomes narrower and longer. To the growth of the overall size of the calcaneum, CA4, CA7, and CA9–CA11 are undergrowth (< 1); CA3 is isometric (~ 1); and CA2, CA5, CA8, and CA12 are overgrowth (> 1) (Table 8). As growing up, the proportion of the calcaneum changes as follows: the body becomes lower except for the tuberosity and does wider, and the tuberosity becomes higher.

Concluding remarks

Here, I investigated intraspecific variations of the various astragalar and calcaneal sizes in living *M. fuscata*. The results will be basic data in interpreting the variations of mammalian astragali and calcanea discovered in paleontological and archaezoological sites.

Acknowledgments

I am grateful to Masanaru Takai, Takeshi Nishimura, and Naoko Egi (Primate Research Institute, Kyoto University, Inuyama, Japan) for graciously providing access to the specimens examined. Thanks are also due to Masahito Natori (Okayama University of Science, Okayama, Japan) and Takashi Okamoto and Nao Kusuhashi (Ehime University, Matsuyama, Japan) for their help in statistical analysis. This manuscript was improved by the reviews of Nao Kusuhashi and Masaya Matsuura (Ehime University, Matsuyama, Japan). This research was supported by the Cooperation Program (2011-A-3, 2012-B-2, and 2013-B-15) of Primate Research Institute (Kyoto University, Inuyama, Japan) and by JSPS KAKENHI Grant Numbers 21770265, 25840172, and 16K07534.

References

Bergqvist, L. P., 2008: Postcranial skeleton of the upper Paleocene (Itaboraian) “Condylarthra” (Mammalia) of Itaboraí Basin, Brazil. *In*, Sargis, E. and Dagosto, M. *eds*., *Mammalian Evolutionary Morphology: A Tribute to Frederick S. Szalay*, p. 107–133. Springer, Dordrecht.

Boyer, D. M. and Bloch, J. I., 2008: Evaluating the mitten-gliding hypothesis for Paromomyidae and Micromomyidae (Mammalia, “Plesiadapiformes”) using comparative functional morphology of new Paleogene skeletons. *In*, Sargis, E. and Dagosto, M. *eds*., *Mammalian Evolutionary Morphology: A Tribute to Frederick S. Szalay*, p. 233–284. Springer, Dordrecht.

Ciochon, R. L., Gingerich, P. D., Gunnell, G. F. and Simons, E. L., 2001: Primate postcrania from the late middle Eocene of Myanmar. *Proceedings of the National Academy of Sciences of the United States of America*, **98**: 7672–7677.

Ciochon, R. L. and Gunnell, G. F., 2004: Eocene large-bodied primates of Myanmar and Thailand: morphological considerations and phylogenetic affinities. *In*, Ross, C. F. and Kay, R. F. *eds*., *Anthropoid Origins: New Visions*, p. 249–282. Kluwer Academic/Plenum Publishers, New York.

Corruccini, R. S., 1983: Principal components for allometric analysis. *American Journal of Physical Anthropology*, **60**: 451–453.

Dagosto, M., Marivaux, L., Gebo, D. L. Beard, K. C., Chaimanee, Y., Jaeger, J.-J., Marandat, B., Soe, A. N.

and Kyaw, A. A., 2010: The phylogenetic affinities of the Pondaung tali. *American Journal of physical Anthropology*, **143**: 223–234.

Dagosto, M. and Terranova, C. J., 1992: Estimating body size of Eocene primates: a comparison of results from dental and postcranial variables. *International Journal of Primatology*, **13**: 307–344.

DeGusta, D. and Vrba, E., 2003: A method for inferring paleohabitats from the functional morphology of bovid astragali. *Journal of Archaeological Science*, **30**: 1009–1022.

Fooden, J. and Aimi, M., 2005: Systematic review of Japanese macaques, *Macaca fuscata* (Gray, 1870). *Fieldiana: Zoology*, 104: 1–200.

Gebo, D. L, and Dagosto, M., 2004: Anthropoid origins: postcranial evidence from the Eocene of Asia. *In*, Ross, C. F. and Kay, R. F. *eds*., *Anthropoid Origins: New Visions*, p. 369–380. Kluwer Academic/Plenum Publishers, New York.

Gebo, D. L., Dagosto, M., Beard, K. C. and Qi, T., 2001: Middle Eocene primate tarsals from China: implications for haplorhine evolution. *American Journal of Physical Anthropology*, **116**: 83–107.

Gebo, D. L., Dagosto, M., Beard, K. C., Qi, T. and Wang, J., 2000: The oldest known anthropoid postcranial fossils and the early evolution of higher primates. *Nature*, **404**: 276–278.

Gebo, D. L., Dagosto, M. and Rose, K. D., 1991: Foot morphology and evolution in early Eocene *Cantius*. *American Journal of Physical Anthropology*, 86: 51–73.

Gray, J. E., 1870: *Catalogue of Monkeys, Lemurs, and Fruit-Eating Bats in the Collection of the British Museum*, viii + 137 p. Trustees of the British Museum (Natural History), London.

Gunnell, G. F. and Ciochon, R. L., 2008: Revisiting primate postcrania from the Pondaung Formation of Myanmar. *In*, Fleagle, J. G., Gilbert, C. C. *eds*., *Elwyn Simons: A Search for Origins*, p. 211–228. Springer, New York.

Gunnell, G. F., Ciochon, R. L., Gingerich, P. D. and Holroyd, P. A., 2002: New assessment of *Pondaungia* and *Amphipithecus* (Primates) from the late middle Eocene of Myanmar, with a comment on ‘Amphipithecidae.’ *Contributions from the Museum of Paleontology, University of Michigan*, **30**: 337–372.

Hébert, D., Lebrun, R. and Marivaux, L., 2012: Comparative three-dimensional structure of the trabecular bone in the talus of primates and its relationships to ankle joint loads generated during locomotion. *The Anatomical Record*, **295**: 2069–2088.

Ihaka, R. and Gentleman, R., 1996: R: a language for data analysis and graphics. *Journal of Computational and Graphical Statistics*, **5**: 299–314.

Jogahara, Y. O., Natori, M., 2013: Talar maturity determined by epiphyseal closure of the calcaneus. *Folia Primatologica*, **84**: 11–17.

Jolicoeur, P., 1963: The multivariate generalization of the allometry equation. *Biometrics*, **19**: 497–499.

Kusuhashi, N. and Okamoto, T., 2015: A nonparametric multimodality test—Silverman’s test—and its introduction into paleontology. *Fossils (The Palaeontological Society of Japan)*, **97**: 23–37. (*in Japanese with English title*)

Marivaux, L., Beard, K. C., Chaimanee, Y., Dagosto, M., Gebo, D. L., Guy, F., Marandat, B., Kyaw-Khaing, Aung-Aung-Kyaw, Myo-Oo, Chit-Sein, Aung-Naing-Soe, Myat-Swe and Jaeger, J.-J., 2010: Talar morphology, phylogenetic affinities, and locomotor adaptation of a large-bodied amphipithecid primate from the late middle Eocene of Myanmar. *American Journal of Physical Anthropology*, **143**: 208–222.

Marivaux, L., Chaimanee, Y., Ducrocq, S., Marandat, B., Sudre, J. Marandat, B., Soe, A. N., Tun, S. T., Htoon, W. and Jaeger J-J., 2003: The anthropoid status of a primate from the late middle Eocene Pondaung Formation (Central Myanmar): tarsal evidence. *Proceedings of the National Academy of Sciences of the United States of America*, **100**: 13173–13178.

Martinez, J.-N. and Sudre, J., 1995: The astragalus of Paleogene artiodactyls: comparative morphology, variability and prediction of body mass. *Lethaia*, **28**: 197–209.

Mouri, T. and Nishimura, T., 2002: Craniometry of adult male Japanese macaques from the Yakushima, Koshima and Kinkazan islands. *Primate Research*, **18**: 43–47. (*in Japanese with English summary*)

Nakatsukasa, M., Takai, M. and Setoguchi, T., 1997: Functional morphology of the postcranium and locomotor behavior of *Neosaimiri fieldsi*, a *Saimiri*-like middle Miocene platyrrhine. *American Journal of Physical Anthropology*, **102**: 515–544.

Natori, M., 2002a: Allometric scaling in platyrrhine molars and relationships between their relative size and loss of the third molar in the Callitrichinae. *Primate Research*, **18**: 59–67. (*in Japanese with English summary*)

Natori, M., 2002b: Allometric scaling in the molars of titi monkeys. *Primate Research*, **18**: 49–57. (*in Japanese with English summary*)

Parr, W. C. H., Chatterjee, H. J. and Soligo, C., 2011: Inter- and intra-specific scaling of articular surface areas in the hominoid talus. *Journal of Anatomy*, **218**: 386–401.

Penkrot, T. A., Zack, S. P., Rose, K. D., and Bloch, J. I., 2008: Postcranial morphology of *Apheliscus* and *Haplomylus* (Condylarthra, Aphelestidae): Evidence for a Paleocene Holarctic origin of Macroscelidea. *In*, Sargis, E. and Dagosto, M. *eds*., *Mammalian Evolutionary Morphology: A Tribute to Frederick S. Szalay*, p. 73–106. Springer, Dordrecht.

Plummer, T. W., Bishop, L. C., Hertel, F., 2008: Habitat preference of extant African bovids based on astragalus morphology: operationalizing ecomorphology for palaeoenvironmental reconstruction. *Journal of Archaeological Science*, **35**: 3016–3027.

Polly, P. D., 2008: Adaptive zones and the pinniped ankle: A 3D quantitative analysis of carnivoran tarsal evolution. *In*, Sargis, E. and Dagosto, M. *eds*., *Mammalian Evolutionary Morphology: A Tribute to Frederick S.*

Szalay, p. 165–194. Springer, Dordrecht.

R Core Team, 2018: R: *A language and environment for statistical computing*. R Foundation for Statistical Computing, Vienna. URL https://www.R-project.org/

Rafferty, K. L., Wlker, A., Ruff, C. B., Rose, M. D. and Andrews, P. J., 1995: Postcranial estimates of body weight in *Proconsul*, with a note on a distal tibia of P. major from Napak, Uganda. *American Journal of Physical Anthropology*, **97**: 391−402.

Seiffert, E. R. and Simons, E. L., 2001: Astragalar morphology of late Eocene anthropoids from the Fayum Depression (Egypt) and the origin of catarrhine primates. *Journal of Human Evolution*, **41**: 577–606.

Shockey, B. J. and Anaya, F., 2008: Postcranial osteology of mammals from Salla, Bolivia (late Oligocene): Form, function, and phylogenetic implications. *In*, Sargis, E. and Dagosto, M. *eds*., *Mammalian Evolutionary Morphology: A Tribute to Frederick S. Szalay*, p. 135–157. Springer, Dordrecht.

Silverman, B. W., 1981: Using kernel density estimates to investigate multimodality. *Journal of the Royal Statistical Society, Series B*, **43**: 97–99.

Silverman, B. W., 1983: Some properties of a test for multimodality based on kernel density estimates. *In*, Kingman, J. F. C. and Reuter, G. E. H., *eds*., *Probability, Statistics and Analysis, London Mathematical Society Lecture Series*, **79**: 248–259. Cambridge University Press, London.

Szalay, F. S., 1977: Phylogenetic relationships and a classification of the eutherian Mammalia. *In*, Hecht, M. K., Goody, P. C. and Hecht, B. M., *eds*., *Major Patterns in Vertebrate Evolution*, p. 315–374. Plenum Press, New York and London.

Tsubamoto, T., 2014: Estimating body mass from the astragalus in mammals. *Acta Palaeontologica Polonica*, **59**: 259–265.

Tsubamoto, T., 2019: Relationship between the calcaneal size and body mass in primates and land mammals. *Anthropological Science*, **127**: 73–80. doi: 10.1537/ase.190221

Tsubamoto, T., Egi, N., Takai, M., Thaung-Htike, and Zin-Maung-Maung-Thein, 2016: Body mass estimation from the talus in primates and its application to the Pondaung fossil amphipithecid primates. *Historical Biology*, **28**: 27–34.

Appendix

Appendix (Table A1 and Figures A1–A3) is available from http://www.sci.ehime-u.ac.jp/wp/research/bulletin/.